PCCP

Accepted Manuscript




ROYAL SOCIETY OF CHEMISTRY

www.rsc.org/pccp

PCCP

COMMUNICATION

# Classical Group Theory adapted to the mechanism of $Pt_3Ni$ nanoparticle growth: the role of $W(CO)_6$ as the "shape-controlling" agent

Received 00th January 20xx,
Accepted 00th January 20xx

DOI: 10.1039/x0xx00000x

www.rsc.org/

M. Radtke and A. Ignaszak*

**Classical group theory was applied to prove the $Pt_3Ni$ crystallographic transformation from Platonic cubic to Archimedean cuboctahedral structures and the formation of $Pt_3Ni$ polypods. The role of $W(CO)_6$ as a shape-controlling agent is discussed in respect to crystallographic features of the cluster and superstructures generated as control samples.**

The colloidal Pt and Pt-based alloys are very important catalysts in chemical and electrochemical processes, including hydrogenation,[1] isomerization,[2] photocatalytic splitting of water,[3] oxygen reduction[4] or methanol oxidation.[5] It has been proven that all Pt-catalysed reactions are sensitive to the crystallographic structure,[6] electronic structure[7] and a surface atomic arrangement[8] of the catalyst and can be controlled by tuning the composition and a shape of nanoparticles. This molecular-scale engineering control generates catalysts with desired and improved functions and is attained in many different ways, such as the surface-energy and surfactant-govern growth,[9] a diffusion-limited growth,[10] atom or particle-mediated growth,[11] defects in seed-induced anisotropic growth,[12] chemical etching of colloidal particles,[13] electrochemistry-driven synthesis,[14] or by using carbonyl-containing organometallics as a reducing agent.[15] Among listed, relatively unexplored is last one, especially important for the fabrication of an ultra-fine metal nanoparticles (particle size less than 20 nm) with desired shapes.[16] In this methods the rate of metal nucleation during particle growth is controlled by a foreign element (metallic or ion) generated in situ during thermal decomposition of e.g., carbonyls (W,[16] Mn[17]). Taking the $W(CO)_6$-mediated synthesis of colloidal Pt as an example, at the critical temperature, the $W^0$ generated from $W(CO)_6$ can reduce the $Pt(acac)_2$ to Pt atoms according to the equilibrium: $Pt^{2+}+W^0 \leftrightarrow W^{n+}+Pt^0$.[18] The tungsten ions may further accumulate locally with variable concentration and influence to the Pt growth. In such case the $Pt(acac)_2$-to-$W^0$ concentration interplay has strong effect on the $Pt^0$ seeds development. The Pt crystal growth will be also strongly affected by operating temperature and the reaction time, and also by the presence of surfactant or an additional reducing agent, as it is in case of $Mn_2(CO)_{10}$-mediated synthesis of Pt nanocrystals.[17] Assuming that the reaction temperature is close to the carbonyl decomposition (but does not exceed) and the chemical reduction of Pt cation is predominant, the second possible mechanism of Pt growth that involves carbonyl groups as the building units for Pt metal (not foreign metal or cation) is expected. This process implicates a mechanism, known as the oriented attachment,[19] in which atoms are preferentially arranged towards specific crystallographic directions of the building units. This occurs in order to minimize the interface energy (in other words, atoms will be preferentially attached to facets with the highest surface energy or surface area).[20] This method is an excellent way of synthesis of the ordered superstructures composed of many individual nanocrystals that share common crystallographic planes. Such structures possess scattering properties similar to those of single crystals.[20a] In this study we aim to synthesize $Pt_3Ni$ clusters or superstructures, which depending on the synthesis conditions, can be generated with controllable features, owing to the presence of the tungsten carbonyl, the shape-controlling agent. The role of metal carbonyl in nanocluster/superstructure synthesis under various conditions (variable temperature, concentration, type of solvent, reaction time, etc.) has been already demonstrated,[16] providing very important insights in optimization of the process that delivers nano-objects with desired architectures. Our approach is to correlate the carbonyl structure with the collective symmetric configurations of metallic nanoparticles using theoretical assumptions. The proposed analysis is based on generalized group theory applied to the point group mutual for interacting (carbonyl – shape controlling agent) and resulting species (metal nanoparticles). In respect to the theoretical arguments, we will prove that irreducible representations responsible for an excitation of translational modes in Cartesian coordinates can be defined by simple geometrical considerations based on a point group character tables, and without advance numerical computations. Based on HR-TEM observations the $Pt_3Ni$ cluster has cuboctahedral features ($O_h$ group[20b]). Thus the formation of such structure can be assumed as the transformation from Platonic cubic into Archimedean cuboctahedral arrangement. Furthermore, the same formalism is

*Institute of Organic and Macromolecular Chemistry, Friedrich-Schiller University, Lessingstrasse 12, 07743 Jena, Germany*
* anna.ignaszak@uni-jena.de

applied to study the combination of the hierarchical arrays composed of a large number of nanoparticles ($Pt_3Ni$ polypods). The details regarding synthesis procedure for cuboctahedral $Pt_3Ni$ and polypods with an elemental mapping are provided in supporting information.

**Theoretical assumption based on group theory**

Energy can be considered as a sum of electronic, translational, rotational and vibrational elements.[21] Energy generated by heat uptake/release (during the temperature change in the system) is defined as random mode of translational kinetic energy in solids and random mode of rotational and translational fractions in gases composed of many atoms.[21] In respect to this, when heat is applied to the molecule/ion/atom (e.g., during the temperature-dependent synthesis of metal particles) its translational modes are excited, resulting in an initiation of the structural transformations.

Fig. 1 represents the $W(CO)_6$ octahedral crystal incorporated into a cube defined by 48 symmetry operations that are categorized by classes: E, 8 $C_3$, 6 $C_4$, 6 $C_2$, 3 $C_2$ (= $C_4^2$), i, 6 $S_4$, 8 $S_6$, 3 $\sigma_h$, 6 $\sigma_d$.[22] Also, since cube and octahedron belong to the point group $O_h$, they both have the same set of symmetry operations.[22] As a result, each can be generated from the other by cutting corners, e.g., irregular polyhedron, which is an intermediate structure, and is called cuboctahedron (and is also affiliated to $O_h$ symmetry). The matrixes that are necessary to create an irreducible representation are listed below:[23a]

$$\mathrm{E}: x, y, z \rightarrow x, y, z \equiv \mathrm{E}\begin{bmatrix}1 & 0 & 0\\ 0 & 1 & 0\\ 0 & 0 & 1\end{bmatrix}\begin{bmatrix}x\\ y\\ z\end{bmatrix} = \begin{bmatrix}x\\ y\\ z\end{bmatrix} \quad (1)$$

$$\mathrm{C_x}(\theta) \qquad \begin{bmatrix}\cos\theta & -\sin\theta & 0\\ \sin\theta & \cos\theta & 0\\ 0 & 0 & 1\end{bmatrix}\begin{bmatrix}x\\ y\\ z\end{bmatrix} \quad (2)$$

$$\mathrm{C_2}: C_2(z, 180°)\begin{bmatrix}-1 & 0 & 0\\ 0 & -1 & 0\\ 0 & 0 & 1\end{bmatrix}\begin{bmatrix}x\\ y\\ z\end{bmatrix} = \begin{bmatrix}-x\\ -y\\ z\end{bmatrix} Character - 1 \quad (3)$$

$$\mathrm{C_3}: (z, 120°) \quad \begin{bmatrix}-0.5 & 0 & 0\\ \sqrt{3}/2 & -0.5 & 0\\ 0 & 0 & 1\end{bmatrix}\begin{bmatrix}x\\ y\\ z\end{bmatrix} = \begin{bmatrix}-0.5x\\ -0..5y\\ z\end{bmatrix} Character\ 0 \quad (4)$$

$$\mathrm{C_4}: \quad C_4(z, 90°)\begin{bmatrix}0 & -1 & 0\\ 1 & 0 & 0\\ 0 & 0 & 1\end{bmatrix}\begin{bmatrix}x\\ y\\ z\end{bmatrix} = \begin{bmatrix}-y\\ x\\ z\end{bmatrix} Character\ 1 \quad (5)$$

The matrices for various $C_2$, $C_3$ and $C_4$ rotations (as they affect general points: *x*, *y*, *z*) will give directly characters for $T_1$ irreducible representation (Table 1). The numbers marked in red are counterparts for the calculation of characters of matrix representations in the Table 1.

The main excitation exhibits in $T_1$ irreducible representation that causes the propagation of translational energy modes towards *xz*, *yz* and *z* directions. This excitation event is responsible for the elongation of the specific crystal faces in a face centred cubic (*fcc*), resulting in the formation of cuboctahedron. The calculations are restricted to O group hence it represents only the translational part of $O_h$ group.

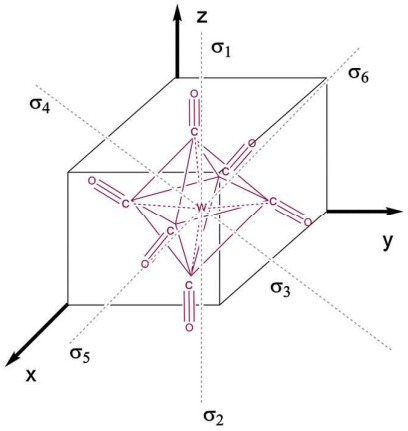


**Fig. 1** The projection of octahedral symmetry group ($O_h$) applied to the $W(CO)_6$ crystal with marked σ bonds.

It is assumed a priori that after applying heat, the Brownian motions of atoms participating in the crystal growth will increase. This leads to the imposition of $O_h$ group to just O, which makes the calculation more restricted and simplified.

**Table 1.** Character table of octahedral point group.[22]

| O | E | $8C_3$ | $6C'_2$ | $6C_4$ | $3C_2 = (C_4)^2$ | linear functions, rotations |
|---|---|---|---|---|---|---|
| $A_1$ | +1 | +1 | +1 | +1 | +1 | - |
| $A_2$ | +1 | +1 | -1 | -1 | +1 | - |
| E | +2 | -1 | 0 | 0 | +2 | - |
| $T_1$ | +3 | 0 | -1 | +1 | -1 | (x, y, z) ($R_x$, $R_y$, $R_z$) |
| $T_2$ | +3 | 0 | +1 | -1 | -1 | - |

**a) Cube-to-cuboctahedra transition**

The transformation of cube-to-cuboctahedron is illustrated in the Fig. 2. It is predicted that the contact edges of octahedron (tungsten hexacarbonyl) are centres of the excitation where the corresponding cubic crystals grow (also in the direction where the edges overlap). As proven by both theoretical and experimental studies, at the similar synthesis conditions, the face-centred cubic $Pt_3Ni$ are favourable. The $Pt_3Ni$ {111} family of crystallographic planes become thermodynamically the most stable (as it is the most electrochemically stable[23b] and the most catalytically active crystallographic facet of the $Pt_3Ni$ cluster[23c-d]). This promotes a rapid elimination of other $Pt_3Ni$ planes (leading in the presence of carbonyl to $Pt_3Ni$ octahedra). The formation of cuboctahedron from the cube is promoted in the presence of metal carbonyl[16] and this transition can be initiated in different ways. One will be the etching of the cube, followed by dissolution in the <111> directions. It can be also the elongation of the cube towards <111> directions.[24] In terms of geometry, the octahedron is a dual polyhedron in respect to cube, which means the vertexes of the octahedron correspond to

the faces of the cube. This explains the formation of the octahedron through the etching of the cube. In such case, the vertex-to-vertex distance of octahedron would be equal the length of edge. The cube is also dual polyhedron in respect to octahedron, taking into account an opposite that the cuboctahedron can grow from cubes. In fact, the cube grows initially into octahedron; therefore the vertex-to-vertex distance of octahedron is two times longer than the length of the cube edge. Based on this assumption, the possible explanation of cube-to-octahedron evolution is that at lower operating temperatures the metal carbonyl will act as the crystal seed for the epitaxial growth of $Pt_3Ni$ cuboctahedron and at higher temperatures (above $W(CO)_6$ decomposition) the metal (or metal ion) will selectively stabilize the Pt (111) species. In the latest case the $W^0$ acts as the reducing agent in $Pt^{2+} + 2e^- = Pt^0$ process. Here, the $Pt^0$ will occupy the position of galvanically replaced $W^0$, similar as for the $Mn_2(CO)_{10}$-assited synthesis.[17] $Mn_2CO_{10}$ belongs to D4d group symmetry and $W(CO)_6$ to $O_h$. The nucleation step controlled by either tungsten hexacarbonyl or dimanganese decacarbonyl starts with the elongation of *x, y* and *z* axis (Fig. 1). An excitation of the specific modes resulting in the growth along these directions is similar for both symmetries. Although, the point groups are different for these carbonyls, both can initiate elongations of the same modes as discussed by other groups.[25-26] As confirmed experimentally in this work, if the process is not quenched, a sub-sequential growth of $Pt_3Ni$ polypods takes place. This was accomplished by annealing the reaction vessel at 230 °C for several hours (Fig. 3).

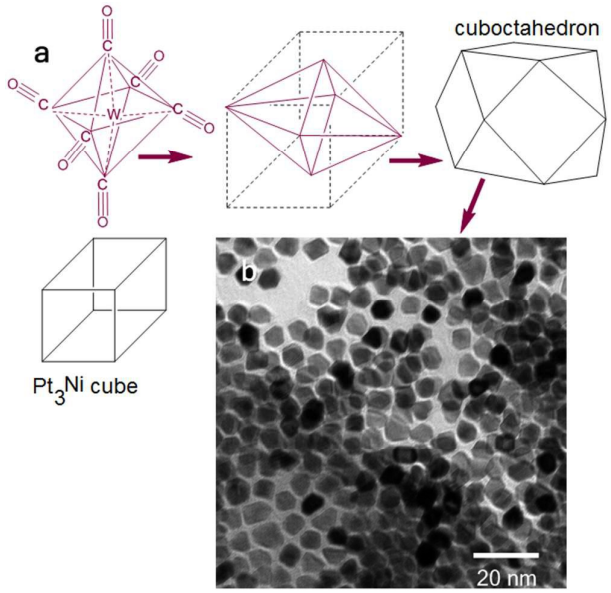


**Fig. 2** Comparison between face centred cube, cuboctahedron and tungsten hexacarbonyl with the point group $O_h$ (a) together with TEM image of $Pt_3Ni$ structures synthetized in this work (b).

**b) Formation of "porous crystals" (polypods)**

For branched metal nanocrystals (tetrapods, octapods, multipods, and hyper-branched nanocrystals), the common synthetic control is a low carbonyl-to-Pt(acac)$_2$ ratio and/or long reaction time.[27] At these experimental conditions the porous crystal growth will be affected by the interplay of carbonyl-to-$Pt^0$ seed local concentration. At the operating temperature of 230 $^oC$, carbonyl is depleted before all Pt precursors are reduced to $Pt^0$, resulting in local gradients of the seed concentration (sometimes called "$Pt^0$ monomer"). These metal monomers are captured by corners of the metal nanocrystals. Due to the local $Pt^0$ depletion, more monomers are generated around the corners and thus corners grow faster. This phenomenon is described as a "branch instability" and explains the crystal growth of porous metallic structures such as snow crystals.[28] The growth of multipods initiated by the local gradient concentration can be classified as a four-step process that includes (steps are graphically displayed in Fig. 3 a): the formation of quasi-octapods (step 1), the transition of quasi octapods to etched octapods (step 2), the transition of etched octapods to porous nanocrystals (step 3) and the growth of porous nanocrystals (step 4), as projected in Fig. 3. During the first phase, the quasi-octapods are generated from single cuboctahedral crystals. During this process faster growth on the {111} facets than on the {100} leads to the prolongation along the <111>. In the second step, the arms of quasi-octapods grow along the <111>, whereas the centre of the {100} facets has been reduced (etched), resulting in the formation of etched-octapods. This process intensifies in step 3: longer branches are generated simultaneously with the intensive etching of the core, resulting in ultra-porous nanocrystals (step 4 in Fig. 3 a).

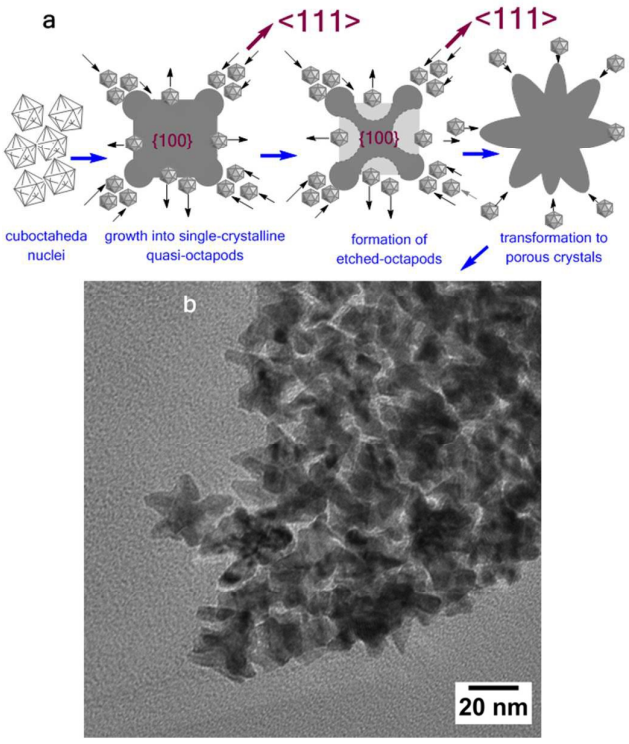

**Fig. 3** The formation of $Pt_3Ni$ polypods from cuboctahedral particles (a) and the corresponding TEM image (b).

## Conclusions

The growth and the shape transformation of $Pt_3Ni$ particles and porous $Pt_3Ni$ superstructures are discussed with respect to the role of $W(CO)_6$ as the shape controlling agent. The transition of $Pt_3Ni$ cubes into cuboctahedral in the kinetically controlled regime (temperature dependent) can proceed according to two mechanisms. First assumes the epitaxial crystal growth over the metal carbonyl template that occurs below the $W(CO)_6$ thermal decomposition. The second path follows the reduction of $Pt^{2+}$ with $W^0$ associated with the preferential $Pt^0$ occupation in the position of galvanically replaced tungsten. The theoretical calculations with assumptions for the $O_h$ group symmetry proved the crystallographic orientation of $Pt_3Ni$. Furthermore, the formation of $Pt_3Ni$ polypod superstructure from cuboctahedral crystals *via* a core crystal etching and the elongation of crystal corner toward the <111> directions were discussed and correlated with experimental results (porous structures that were generated at higher temperatures or at extended reaction time). Since Pt-based alloys have great application potential in catalysis or the structure-sensitive reactions we believe that this theoretical approach provides some insights in designing of other multimetallic systems and highlights the important role of the shape controlling additives.

## Acknowledgements

We thank Dr. Stephanie Höppener for TEM imaging and Carl Zeiss Foundation for the financial support.

## Notes and references


1 X. Li, B. Li, M. Cheng, Y. Du, X. Wang and P. Yang, *J. Molec. Catal. A,* 2008, **284**, 1.
2 B. Rezaei, M. Mokhtaranpour and A. A. Ensafi, *Int. J. Hydr. Energ.,* 2015, **40**, 6754.
3 F. Mauriello, E. Garrone, M. G. Musolino, R. Pietrapaolo and B. Onida, *Mol. Catal. A,* 2010, **328**, 27.
4 N. V. Long, T. D. Hien, T. Asaka, M. Ohtaki and M. Nogami, *Int. J. Hydr. Energ.,* 2011, **36**, 8478.
5 M. C. Figueirendo, J. Solla- Gullón, F. J. Vidal- Iglesias, M. Nisula, J. M. Feliu and T. Kallio, *Electrochem. Commun.,* 2015, **55**, 47.
6 E. Florez, F. Mondragon and F. Illas, *Surface Science,* 2012, **606**, 1010.
7 M. D. Kane, F. S. Roberts and S. L. Anderson, *International Journal of Mass Spectrometry,* 2015, **377**, 263.
8 L. C. Wang, C. Y. Huang, C. Y. Chang, W. C. Lin and K. J. Chao, *Microporous and Mesoporous Materials,* 2008, **110**, 451.
9 S. K. Mehta, S. Kumar and M. Gradzielski, *Journal of Colloid and Interface Science,* 2011, **360**, 497.
10 L. Ottaviano, P. Parisse, V. Grossi and M. Passacantando, *Journal of Non-Crystalline Solids,* 2010, **356**, 2076.
11 T. Wang, S. Li, M. Jia, C. Guo and J. Hu, *Colloids and Surfaces A: Physicochem. Eng. Aspects,* 2013, **434**, 229.
12 L. Han, P. Cui, H. He, H. Liu, Z. Peng and J. Yang, *Journal of Power Sources,* 2015, **286**, 488.
13 Y. Zheng, Y. Wang, S. Wang and C. H. A. Huan, *Colloids and Surfaces A: Physicochem. Eng. Aspects,* 2006, **277**, 27.
14 M. Radtke, S. Stumpf, B. Schröter, S. Höppener, U. S. Schubert and A. Ignaszak, *Tetrahedron Lett.,*2015, in press
15 Y. Luo, J. M. Mora-Hernández, L. A. Estudilo-Wong, E. M. Arce-Estrada and N. Alonso-Vante, *Electrochim. Acta,* 2015, **173**, 771.
16 J. Zhang, H. Yang, J. Fang and S. Zou, *Nano. Lett.,* 2010, **10**, 638.
17 Y. Kang, J. B. Pyo, X. Ye, R. E. Diaz, T. R. Gordon, E. A. Stach and B. Murray, *ACS Nano,* 2013, **7**, 645.
18 J. Zhang and J. Fang, *J. Am. Chem. Soc.*, 2009, **131**, 18543.
19 K. A. Fichthorn, *Chemical Engineering Science,* 2015, **121**, 10.
20 (a) C. Luna, E.D. Barriga-Castro and R. Mendoza-Reséndez, *Acta Materalia*, 2014, **66**, 405; (b) D. Bonchev, *Chemical Group Theory: Techniques and Applications*, Taylor & Francis, 1995, ISBN-10:2884490345.
21 P. Atkins and J. de Paula, *Physical Chemistry*, 9th Ed., OUP Oxford, 2010, ISBN-13: 978-1429218122.
22 F. A. Cotton, *Chemical Applications of Group Theory*, 3rd Ed., Wiley-Interscience; ISBN-10: 0471510947.
23 (a) G. H. Wagniére, *On Chirality and the Universal Asymmetry: Reflections on Image and Mirror Image*, John Wiley & Sons, ISBN: 978-3-90639-038-3; (b) J. Fang and J. Zhang, 2014, US patent US8741801 B2; (c) V. R. Stamenkovic, B. Fowler, B. S. Mun, G. Wang, P. N. Ross, S. A. Lucas and N. M. Markovic, *Science*, 2007, **315**, 493; (d) N. Todoroki, Y. Lijima, R. Takahashi, Y. Asakimori and T. Wadayama, *J. Electrochem. Soc.*, 2013, **160**, F591.
24 S. C. Yang, F. Hong, L. Q. Wang, S. W. Guo, X. P. Song, B. J. Ding and Z. M. Yang, *J. Phys. Chem. C*, 2010, **114**, 203.
25 A. Gholami and A. Reza Ashrafi, *Indian Journal of Chemistry*, 2008, **47A**, 225.
26 J. B. Westmore, K. J Fisher and G. D. Willett, *Int. J. Mass Spectr.*, 1999, **182-183**, 53.
27 L. Xiong and T. He, *Electrochem. Commun.,* 2006, **8**, 1671.
28 J. Gravner and D. Griffeath, *Physica D: Nonlinear Phenomena,* 2008, **237**, 385.